



Automated temperature-responsive deep eutectic solvent microextraction for rapid determination of synthetic dyes in food samples

Alesia Gerasimova^a, Anoop Kishore Vatti^b, Tamal Banerjee^c, Andrey Shishov^{a,*} 

^a Saint Petersburg State University, Universitetskaya Emb. 7/9, 199034, St Petersburg, Russia

^b Department of Chemical Engineering, Manipal Institute of Technology (MIT), Manipal Academy of Higher Education (MAHE), Manipal, Karnataka, 576104, India

^c Department of Chemical Engineering, Indian Institute of Technology Guwahati, Assam, 781039, India

ABSTRACT

A automated microextraction method based on temperature-responsive deep eutectic solvents (TRDESs) was developed for the determination of synthetic dyes in food samples. The system employs a homogeneous aqueous TRDES solution, composed of lidocaine and heptanoic acid (1:1 mol/mol), which acts both as extraction medium and as a thermally induced phase-separating agent. Upon heating above the lower critical solution temperature, spontaneous phase separation occurs, allowing direct collection of the enriched TRDES phase without centrifugation or manual handling. The entire process from sample introduction to extract collection is integrated into a programmable flow-based platform. The method was optimized and validated for four banned synthetic dyes: Rhodamine 6G, Sudan I, II, and III. Good linearity (0.025–100 mg L⁻¹), low limits of detection (0.001–0.008 mg L⁻¹), and high intra-/inter-day precision (RSDs: 2–7 %) were achieved. Real beverage samples were successfully analyzed, and spiked recoveries showed good agreement with a reference DLLME method (relative bias: 1–5 %). All steps were performed without the use of toxic organic solvents or centrifugation. Molecular dynamics simulations confirmed that π - π stacking and van der Waals interactions between rhodamine and lidocaine govern the extraction mechanism. Additionally, the green performance of the method was assessed using AGREEprep and ComplexGAPI, demonstrating high environmental sustainability. Overall, the proposed method offers a robust, automated, and environmentally friendly solution for trace-level screening of banned dyes in complex food matrices.

1. Introduction

Deep eutectic solvents (DESs) [1,2] have gained substantial attention as sustainable alternatives to conventional organic solvents due to their low volatility [3], tunable physicochemical properties [4], and straightforward preparation [5]. Among these, temperature-responsive deep eutectic solvents (TRDESs) constitute a promising subclass capable of undergoing reversible phase transitions triggered by mild temperature changes. This feature enables selective extraction and simplified recovery of analytes without the use of auxiliary dispersive or demulsifying agents [6]. The temperature-responsive behavior of TRDESs has facilitated the development of homogeneous liquid–liquid microextraction (HLLME) procedures.

In general, TRDESs can be categorized as lower critical solution temperature (LCST)-type or upper critical solution temperature (UCST)-type systems. In LCST-type systems, the solvent and water are completely miscible at lower temperatures but separate into two phases upon heating above a defined threshold. Conversely, UCST-type systems remain immiscible at lower temperatures and become homogeneous only upon heating. The nature and molar ratio of the hydrogen bond

donor (HBD) and acceptor (HBA) determine whether a TRDES exhibits LCST or UCST behavior, as well as the corresponding phase transition temperature [7,8].

Recent studies have highlighted the versatility of TRDESs in various extraction applications. For example, Bian et al. developed an ultrasound-assisted TRDES system based on ethanolamine and o-cresol to extract pyrethroid pesticides from soil, achieving recoveries up to 94 % and maintaining performance over five reuse cycles [9]. Similarly, Shen et al. reported ternary LCST-type TRDESs applied to carotenoid extraction from tomatoes, where phase separation was induced at 68 °C and enabled high yields of lycopene and β -carotene while maintaining green chemistry criteria [10]. Another notable study reported the *in-situ* formation of TRDES microdroplets for extracting bisphenols from beverages, achieving high enrichment factors with simplified phase separation using disposable pipette-based formats [11].

The fundamental mechanism of TRDES operation is governed by temperature-induced shifts in acid–base equilibria and hydrogen bonding networks. For instance, in lidocaine-based systems, increasing the temperature decreases ionization and hydrophilicity, leading to spontaneous liquid–liquid phase separation [8,12]. These thermally

This article is part of a special issue entitled: separative instrumental analysis published in Talanta.

* Corresponding author.

E-mail address: a.y.shishov@spbu.ru (A. Shishov).

<https://doi.org/10.1016/j.talanta.2025.129029>

Received 17 July 2025; Received in revised form 30 September 2025; Accepted 23 October 2025

Available online 30 October 2025

0039-9140/© 2025 Elsevier B.V. All rights reserved, including those for text and data mining, AI training, and similar technologies.

responsive properties have been utilized to extract both hydrophobic and hydrophilic compounds, enabling the development of greener, more efficient, and recyclable extraction workflows.

Despite the growing interest in TRDESs, most reported applications rely on manual protocols involving operator-controlled heating and manual phase recovery [9–11]. Manual separation of TRDES and aqueous phases is technically challenging, especially at elevated temperatures, where centrifugation increases the risk of analyte loss and contamination.

To the best of our knowledge, no automated platform integrating TRDES preparation, temperature-induced phase separation, and extract recovery into a programmable flow system has been reported. The automation of such workflows opens broad opportunities in chemical analysis [13,14] by enabling higher throughput [15], improving reproducibility, reducing operator exposure to heated phases, and facilitating integration with downstream analytical instruments. Overall, the use of deep eutectic solvents in flow-based analytical systems remains underexplored [16,17].

This study addresses the existing gap by presenting the first automated microextraction platform based on homogeneous aqueous TRDESs. This system was developed to combine in a single workflow all critical operations, including sample introduction, precise solvent dosing, controlled heating for phase separation, and automated collection of the extract without manual intervention. As a proof of concept, the platform was applied to the determination of banned synthetic dyes (Rhodamine 6G and Sudan I–III) in food samples.

This work reports the first automated homogeneous liquid–liquid microextraction method using a temperature-responsive deep eutectic solvent. The system integrates solvent dosing, temperature-controlled phase separation, and extract recovery into a programmable flow platform. The developed method was optimized, validated, and successfully applied to the determination of banned synthetic dyes in beverages. The approach demonstrated linearity, low detection limits, and good reproducibility, while eliminating toxic organic solvents and centrifugation. The analytical significance of this study lies in providing a green, reproducible, and high-throughput solution for routine food safety monitoring. Following extraction, the analytes were determined by liquid chromatography with diode-array detection, ensuring reliable quantification and selectivity.

2. Experimental

2.1. Reagents and solutions

All chemicals were of analytical grade or higher and used without further purification. Ultrapure water (18 M Ω cm) was obtained from a Milli-Q system (Millipore, USA). Heptanoic acid ($\geq 99\%$) and Rhodamine 6G (certified standard) were purchased from Sigma-Aldrich (Germany). Sudan I, II, and III (certified standards, $\geq 98\%$) were obtained from Vecton (Russia). Lidocaine ($\geq 98\%$) was supplied by Mahendra Chemicals (India). Sodium chloride (analytical grade) was obtained from Lenreaktiv (Russia). Acetonitrile (HPLC grade) was purchased from J.T. Baker (USA). Chloroform ($\geq 99.5\%$) and acetone ($\geq 99.8\%$) were obtained from Vekton (Russia). Methanol (HPLC grade), phosphoric acid ($\geq 85\%$) used for mobile phase preparation and equipment cleaning, were obtained from Merck (Germany).

Stock solutions (1.0 g L $^{-1}$) were prepared by dissolving accurately weighed amounts of each dye in acetonitrile in 25 mL volumetric flasks. The solutions were stored in amber glass bottles at 5 °C and remained stable for at least one month. Working solutions were freshly prepared before each experiment by diluting the stock solutions with acetonitrile.

The target analytes in this study were Rhodamine 6G and Sudan I–III. These dyes were selected as model analytes due to their regulatory importance and physicochemical diversity, thereby demonstrating the method's broad applicability [18,19]. Rhodamine 6G was included as a representative water-soluble dye [20], whereas Sudan I–III, being

weakly polar and sparingly soluble, were chosen to highlight the versatility of the developed TRDES-based extraction system [21].

2.2. Preparation of TRDES

The TRDES was prepared by mixing lidocaine and heptanoic acid (1:1 mol/mol) in a 50 mL glass beaker. The mixture was heated at 60 °C on a magnetic stirrer hot plate (IKA C-MAG HS7, Germany) with continuous stirring at 600 rpm until a clear, homogeneous liquid was formed. The resulting TRDES was stored in sealed glass vials at room temperature and used within two weeks.

2.3. Instrumentation

Chromatographic analyses were performed on an HPLC system LC-20 Prominence (Shimadzu, Kyoto, Japan) equipped with a binary solvent delivery module, an autosampler (SIL-20A), a column oven (CTO-20A), and a photodiode array (PDA) detector (SPD-M20A). The separation was achieved on a Luna C18 analytical column (150 \times 4.6 mm i. d., 5 μ m particle size; Phenomenex, USA). The system control and data acquisition were carried out using LabSolutions software version 5.82 (Shimadzu, Japan). ATR-FT-IR spectra were recorded using an IR Affinity-1 spectrometer with Shimadzu's proprietary software (Shimadzu, Japan). Differential scanning calorimetry (DSC) were performed using a DSC 214 Polyma system (NETZSCH, Germany) under nitrogen flow at a heating rate of 5 °C \cdot min $^{-1}$. The pH measurements were conducted with a PH2101 pH-meter (LOIP, Russia). The automated extraction platform (TRDES-HLLME manifold) consisted of an 8-way rotary injection valve (Cole-Parmer, USA) for sample selection and transfer, a MasterFlex L/S peristaltic pump (Cole-Parmer, USA) with variable speed control was employed, operated through its original proprietary software to ensure precise dosing of samples and reagents, a TW-2 thermostatic water bath (ELMI, Latvia) providing constant temperature control with an accuracy of ± 0.2 °C, and a custom-fabricated extraction chamber constructed from a 10 mL polypropylene pipette tip. All polytetrafluoroethylene (PTFE) tubing (1 mm i.d.) and connectors were thoroughly rinsed with ethanol and ultrapure water before use to prevent cross-contamination.

2.4. Samples

Representative beverage samples (cherry juice, tonic water, and lemonade) were procured from local supermarkets in Saint Petersburg, Russia. All samples were stored in their original sealed plastic containers at ambient temperature (20–25 °C) and were analyzed within four weeks of purchase. Prior to analysis, carbonated beverages were degassed to remove dissolved gases that could interfere with extraction efficiency. Degassing was performed by ultrasonication for 15 min at room temperature (approximately 22 °C) in the ultrasonic bath. After degassing, samples were allowed to equilibrate to room temperature before spiking and extraction. For spiking experiments, known volumes of working dye solutions were pipetted into 50 mL volumetric flasks containing beverage samples to achieve final concentrations ranging from 0.005 to 0.5 mg L $^{-1}$. The mixtures were homogenized by gentle inversion and allowed to stand for 10 min before analysis.

2.5. TRDES-HLLME procedure

The automated homogeneous liquid–liquid microextraction with TRDES was performed according to the following protocol (Fig. 1). First, the selection valve was switched to position 1, and 6.0 mL of the beverage sample were aspirated into the extraction chamber thermostated at 80 °C at a pump flow rate of 5 mL min $^{-1}$ (maximum). The valve was then switched to position 7, and 2.0 mL of an aqueous 28 % (w/v) NaCl solution were introduced at 5 mL min $^{-1}$, yielding in situ an 8.0 mL working solution with a final salt concentration of 7 % (w/v).

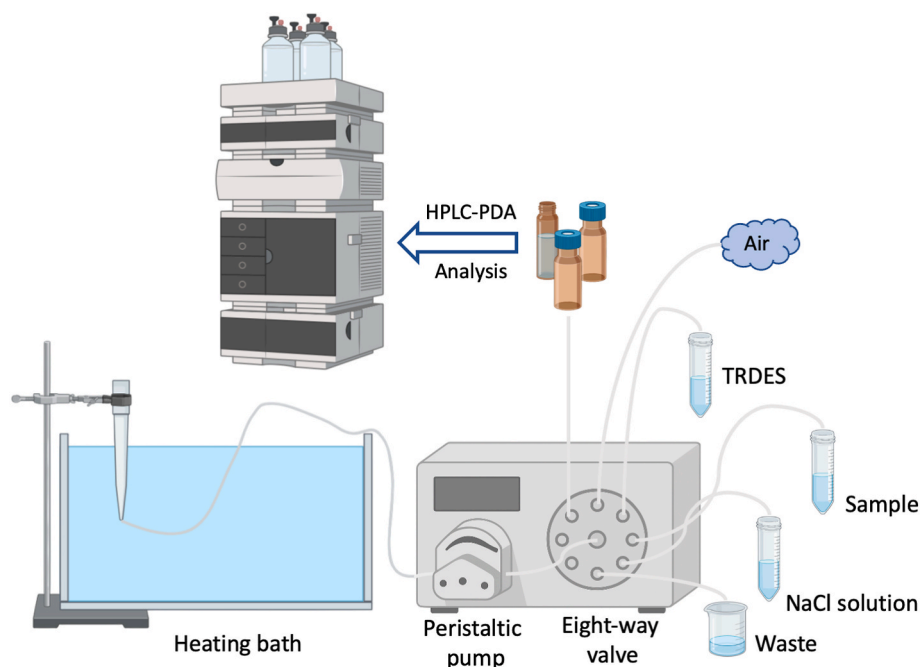


Fig. 1. Schematic representation of the automated homogeneous liquid–liquid microextraction system (TRDES-HLLME) integrated into a programmable flow-based manifold. The setup includes peristaltic pump, sample injection valve and thermostated pipette-tip chamber.

Subsequently, the valve was set to position 2 and 250 μL of TRDES were introduced at a reduced flow rate of 1 mL min^{-1} to accommodate the higher viscosity of the solvent. To promote efficient mixing, the valve was switched to position 3 and air was supplied at 5 mL min^{-1} for 2 min, ensuring dispersion and thermal equilibration of the liquids. Extraction was then allowed to proceed for an additional 10 min under constant temperature and bubbling conditions (at 80 $^{\circ}\text{C}$). During this period, the system transitioned to the two-phase state as the temperature exceeded the LCST of the TRDES mixture. After completion of the extraction step, the valve was turned to position 4 and the aqueous phase was discharged to waste at 5 mL min^{-1} . Subsequently, the valve was set to position 5 and the enriched TRDES phase ($\sim 200 \mu\text{L}$) was automatically transferred into a clean 1.5 mL glass vial at 1 mL min^{-1} for chromatographic analysis. Finally, the valve was switched to position 6, and the system was rinsed three times with 10 mL of ultrapure water at 5 mL min^{-1} to prevent carryover between runs (ESM Table 1). The total preparation time per cycle, including extraction, phase separation, solvent collection, and cleaning, was approximately 20 min. Although the volume of the TRDES phase was not measured directly after extraction, the collected extract was always sufficient for LC analysis; owing to the automated workflow, the recovered solvent volume remained constant across runs, ensuring reproducibility of the method.

2.6. HPLC-PDA procedure

Chromatographic conditions were adapted from previous study on Sudan dye determination [17]. Chromatographic separation was performed at 50 $^{\circ}\text{C}$ on the Luna C18 column. The injection volume was set at 20 μL . The mobile phase consisted of solvent A (1 % phosphoric acid in water) and solvent B (a mixture of acetonitrile and methanol in a ratio of 2:1, v/v). The gradient elution program started with 65 % solvent B from 0 to 5 min, followed by a linear increase to 95 % B from 5 to 10 min, then an isocratic hold at 95 % B between 10 and 20 min, a linear decrease back to 65 % B from 20 to 25 min, and a final hold at 65 % B from 25 to 30 min. The flow rate was maintained at 0.65 mL min^{-1} throughout the run. The PDA detector recorded spectra in the range of 200–600 nm, with quantification performed at 490 nm for Sudan dyes and at 525 nm for Rhodamine 6G. Retention times of the analytes were

confirmed by analyzing standard solutions under identical conditions. Under the optimized chromatographic conditions, the retention times for the four dyes were as follows: Rhodamine 6G – 3.82 min, Sudan I – 12.63 min, Sudan II – 14.52 min, and Sudan III – 17.51 min.

2.7. Reference procedure

For comparison, a dispersive liquid-liquid microextraction (DLLME) method was applied, adapted from Biparva et al. [22]. In this protocol, 3.0 mL of aqueous sample was placed into a 5 mL polypropylene centrifuge tube. A 0.66 mL mixture composed of acetone (disperser solvent) and chloroform (extraction solvent) in a volume ratio of 3:2 was rapidly injected using a 1 mL syringe, resulting in the formation of a cloudy dispersion. The mixture was centrifuged at 3000 rpm for 5 min to separate phases. The lower organic phase (200 μL) was carefully collected with a glass microsyringe and evaporated to dryness in an oven at 75 $^{\circ}\text{C}$. The residue was reconstituted in 500 μL of acetonitrile and transferred into HPLC vials for analysis under the same chromatographic conditions described above.

2.8. Computational details

The explicit rhodamine 6G, henceforth referred to as rhodamine, DES (lidocaine/heptanoic acid) in a 1:1 M ratio, and water molecules are seen as building a liquid-liquid structure, as illustrated in Fig. 2 (a) and (b) and number of molecules used in molecular simulations in Table 1. The DESMOND MD [23] tool is employed for all molecular dynamics (MD) simulations in the Schrödinger simulation software in Schrödinger release 2024-2. For the integration of Newton's equations of motion, we use a time step of 2 fs in all of our simulations. A 9 \AA cut-off distance was used. We employed Optimized Potentials for Liquid Simulations (OPLS4) force fields [24] to precisely represent the bonded and Lennard-Jones interactions. Particle Mesh Ewald (PME) [25,26] was employed for electrostatics. The simulation protocol employed across all systems is explained in the following steps: NPT molecular dynamics simulations are performed for 10 ns to get the average volumes and densities. In order to carry out the NPT simulation, a temperature of 300 K and a pressure of 1 atm are selected. The Nose-Hoover thermostat and

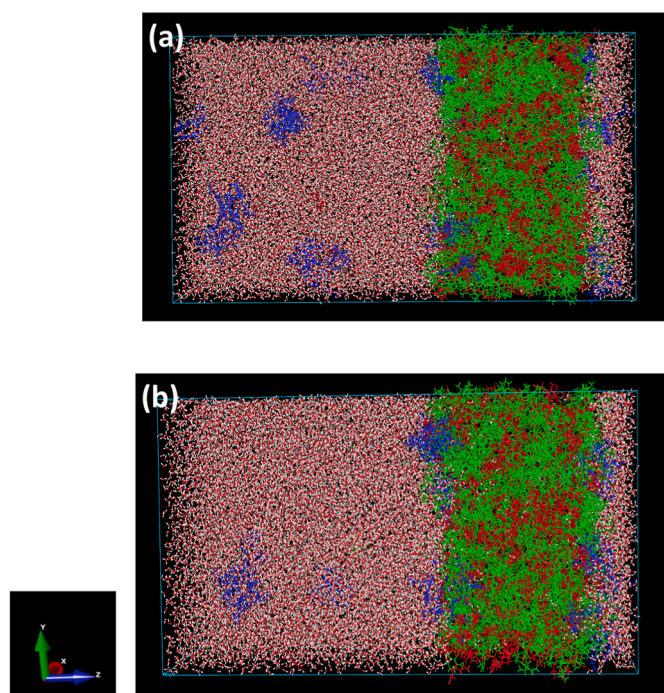


Fig. 2. Snapshots of the NVT MD run aqueous phase and DES phase (a) 1.64 ns of production run (b) 84.83 ns of production run: oxygen is red and hydrogen is white, green molecules are lidocaine, red molecules are heptanoic acid, blue molecules are rhodamine. (For interpretation of the references to color in this figure legend, the reader is referred to the Web version of this article.)

the Martyna-Tobias-Klein barostat, which have coupling constants of 1 ps and 2 ps, respectively, were used to keep the temperature and pressure constant. A production run of 100 ns in the NVT ensemble is subsequently performed and assessed. Our simulations have examined aqueous solution samples containing 1 wt % and 5 wt % rhodamine.

Only one analyte, Rhodamine 6G, was selected for MD simulations. This decision was made to keep the main emphasis of the study on automation. Rhodamine 6G was chosen as the more polar analyte compared to Sudan dyes, which are weakly polar and more readily extracted into nonpolar TRDES. Modeling Rhodamine therefore provided more informative insights into specific solute–solvent interactions without shifting the focus away from the automated workflow.

3. Results and discussion

3.1. Preliminary studies and characterization of TRDES by DSC and ATR-FT-IR

In the present study, a temperature-responsive deep eutectic solvent based on lidocaine and heptanoic acid (1:1 mol/mol) was used. This composition was selected in accordance with previous findings [11], which demonstrated that the equimolar mixture uniquely provides a stable and homogeneous phase through complete acid–base interaction, thereby ensuring phase stability and reproducible extraction

performance in TRDES-HLLME. Non-equimolar systems (2:3 and 3:2) led to the formation of colloidal dispersions due to excess unreacted precursors, which tend to separate into a distinct phase. Heptanoic acid was chosen as the hydrogen bond donor due to its suitable chain length, which provides a balance between hydrophobicity and fluidity, enabling effective phase separation upon heating while maintaining sufficient solvent compatibility with the aqueous phase. Despite its promising properties, this TRDES has not been previously applied in automated sample preparation systems. The present study represents the first attempt to integrate lidocaine/heptanoic acid TRDES into an automated HLLME workflow, combining the advantages of phase-switchable extraction with flow-based analysis for improved reproducibility and analytical efficiency.

To verify the successful formation of the lidocaine/heptanoic acid TRDES and its stability during the extraction procedure, ATR-FT-IR spectroscopy was employed. The spectra of pure lidocaine, heptanoic acid, water, and the TRDES phase before and after TRDES-HLLME are presented in ESM Fig. 1. In the spectrum of heptanoic acid, the characteristic –OH stretching band at 3064 cm^{-1} undergoes a marked red shift to $2859\text{--}2930\text{ cm}^{-1}$ in the TRDES, both before and after microextraction, overlapping with the –CH stretching region. Similarly, the C=O stretching vibration of heptanoic acid appears at 1706 cm^{-1} in the pure compound but shifts to 1687 cm^{-1} in the TRDES, indicating weakening of the hydroxyl bond and confirming hydrogen bond formation between the hydroxyl group of heptanoic acid and the amine nitrogen of lidocaine. For lidocaine, the C–N–H stretching at 3261 cm^{-1} and the –NH bending at 763 cm^{-1} remain unchanged in the TRDES spectra, demonstrating that the amide moiety of lidocaine does not participate in hydrogen bonding. Finally, the broad –OH band of water observed at 3445 cm^{-1} becomes evident in the TRDES phase collected after the TRDES-HLLME process, confirming the presence of residual water.

To further confirm TRDES formation, differential scanning calorimetry experiments were conducted. Samples of 5 mg of pure lidocaine, heptanoic acid, and the prepared TRDES were placed into aluminum crucibles and subjected to a cooling–heating cycle (cooling to $-70\text{ }^{\circ}\text{C}$ followed by heating to $80\text{ }^{\circ}\text{C}$ at a rate of 5 K min^{-1}). The DSC thermograms of pure lidocaine and heptanoic acid exhibited distinct melting peaks at $68\text{ }^{\circ}\text{C}$ and $-9\text{ }^{\circ}\text{C}$, respectively, which is consistent with the behavior of pure crystalline compounds. In contrast, the lidocaine/heptanoic acid mixture did not display any sharp melting peaks within the studied range. Instead, the thermogram showed the absence of well-defined crystallization or melting transitions, indicating that the system is not crystalline and that potential crystallization occurs far below $-70\text{ }^{\circ}\text{C}$. This behavior is characteristic of deep eutectic solvents, thereby confirming that the lidocaine:heptanoic acid (1:1 mol/mol) mixture forms a genuine TRDES rather than a simple binary mixture (ESM Fig. 2).

3.2. Optimization of automated microextraction procedure

In accordance with the developed procedure, 8 mL of an aqueous model solution containing the target dyes (1 mg L^{-1}) was automatically delivered into a pipette tip using a peristaltic pump. The model solution was prepared by diluting $100\text{ }\mu\text{L}$ of a 1 g L^{-1} stock solution of the dyes in

Table 1

Number of rhodamine, lidocaine, heptanoic acid, and water molecules, and simulation box sizes used in MD calculations.

Liquid-Liquid Extraction	Number of Rhodamine Molecules	Number of water molecules	Hydrophobic DES		Simulation Box Size (\AA^3)
			Number of Lidocaine molecules	Number of Heptanoic Acid	
Aqueous Rhodamine (1 wt%) + DES	8	19992	500	500	$72.9 \times 69.6 \times 182.9$
Aqueous Rhodamine (5 wt%) + DES	40	19960	500	500	$73.4 \times 86.0 \times 149.6$

acetonitrile with deionized water. After loading the sample solution, the flow path was switched to introduce 250 μL of TRDES (lidocaine:heptanoic acid 1:1, mol/mol) into the tip. The extraction system was mixed by air bubbling and heating for a standard duration of 12 min, unless otherwise stated. After the extraction was completed, the lower aqueous phase was removed using the pump, and the upper TRDES-phase was automatically transferred to a chromatographic vial for further HPLC-PDA analysis according to 2.5. Key parameters such as TRDES volume, heating time and temperature, salting-out agent concentration and pH of aqueous phase were evaluated.

3.2.1. Effect of TRDES volume and temperature

To investigate the temperature-induced phase transition behavior of the selected temperature-responsive deep eutectic solvent, a series of experiments was conducted using a fixed sample volume of 8 mL. This volume was chosen based on the internal capacity of the 10 mL polymer pipette tip, which served as the extraction vessel in all experiments. To this fixed volume of aqueous model solution, containing the target analytes, varying amounts of TRDES (composed of lidocaine and heptanoic acid in a 1:1 M ratio) were added: 100, 150, 200, 250, 300, and 350 μL . Each mixture was mixed by bubbling and heated at controlled temperatures ranging from 30 $^{\circ}\text{C}$ to 80 $^{\circ}\text{C}$, and the visual appearance and phase behavior of the system were systematically monitored. The main criterion for evaluation was the formation of a temperature-

induced phase transition, i.e., a switch from a homogeneous solution to a biphasic system upon heating.

At TRDES volumes of 100 and 150 μL , the mixtures remained fully homogeneous throughout the entire temperature range (30–80 $^{\circ}\text{C}$), with no observable phase separation. For the mixture containing 200 μL of TRDES, homogeneous solutions were observed at 30–60 $^{\circ}\text{C}$, while partial turbidity began to develop at 70 and 80 $^{\circ}\text{C}$, indicating the onset of demixing, but without distinct phase boundaries. When the TRDES volume was increased to 250 μL , the system remained homogeneous at 30 and 40 $^{\circ}\text{C}$, while at 50, 60, and 70 $^{\circ}\text{C}$, clear phase separation began to occur. Notably, at 80 $^{\circ}\text{C}$, a well-defined biphasic system was observed with a distinct interface between the hydrophobic TRDES phase and the aqueous layer, allowing for reliable extractant recovery. In contrast, with 300 and 350 μL of TRDES, phase separation occurred throughout the entire temperature range (30–80 $^{\circ}\text{C}$), and no homogeneous-to-heterogeneous transition upon heating was observed. The TRDES formed a separate phase regardless of temperature, which is undesirable for temperature-controlled extraction systems relying on solubilization-triggered partitioning. Based on these observations, the combination of 8 mL aqueous sample, 250 μL of TRDES, and an extraction temperature of 80 $^{\circ}\text{C}$ was selected as optimal for subsequent microextraction experiments. Under these conditions, the system undergoes a distinct and reproducible temperature-induced phase separation, ensuring efficient analyte transfer into the TRDES phase and facilitating precise phase

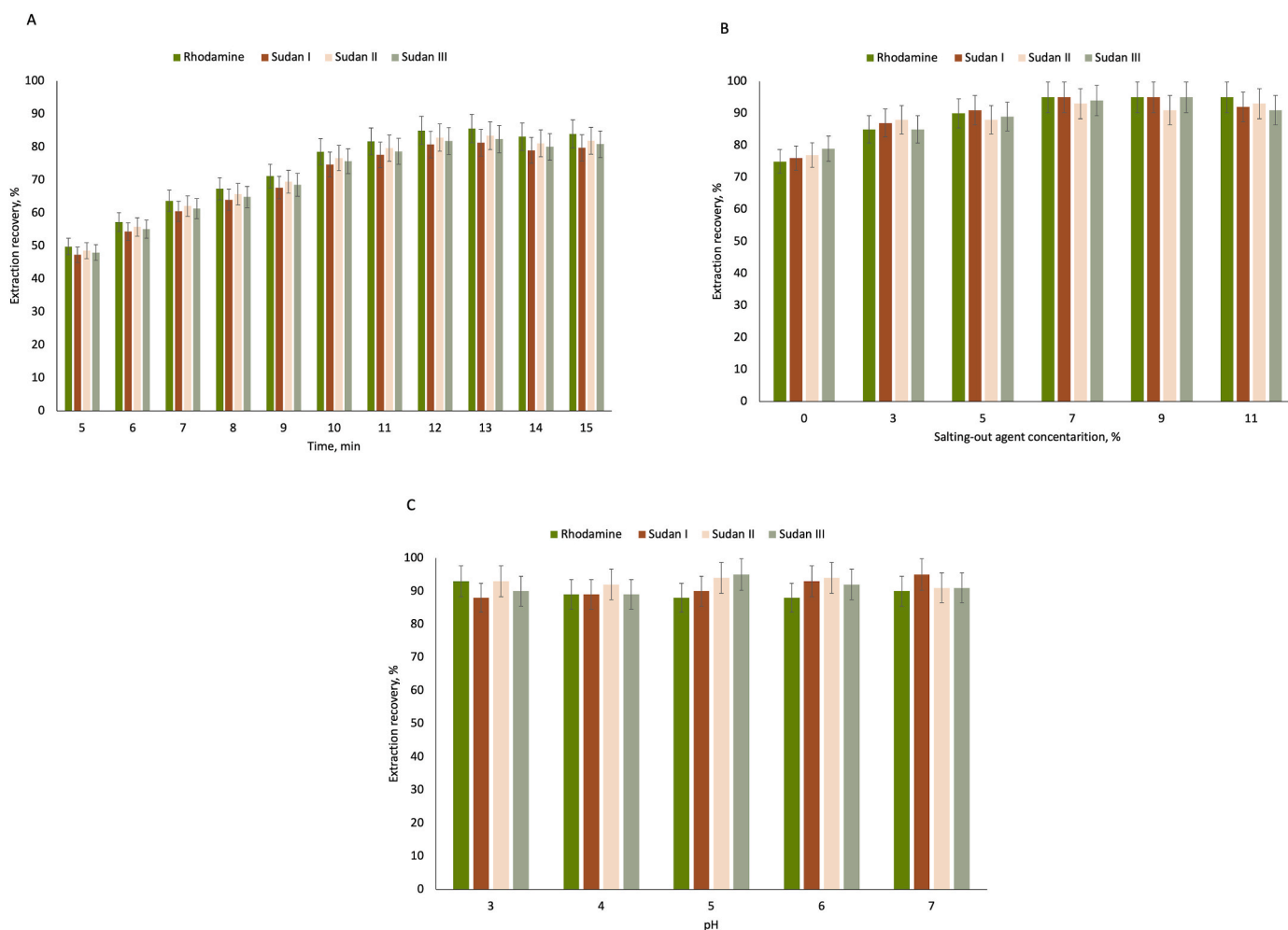


Fig. 3. Effect of experimental parameters on the extraction recovery of rhodamine 6G and Sudan dyes during automated TRDES-HLLME (Dyes concentration 1 mg L^{-1} , 8 mL aqueous sample volume, 250 μL lidocaine/heptanoic acid TRDES (1:1 mol/mol), extraction temperature 80 $^{\circ}\text{C}$, air bubbling-assisted mixing, $n = 3$). (A) Effect of heating time (5–15 min) at 80 $^{\circ}\text{C}$ on extraction recovery. (B) Effect of sodium chloride concentration (0–9 % w/v) on extraction recovery. (C) Effect of aqueous phase pH (3–7) on extraction recovery.

collection for chromatographic analysis.

3.2.2. Effect of heating time

The heating time of the TRDES-HLLME procedure affects the extraction efficiency and the kinetics of mass-transfer equilibrium between the aqueous phase and the TRDES phase. To investigate this effect, the extraction system was heated at 80 °C for 5 to 15 min in 1 min increments. Results show that the extraction recovery of the analytes gradually increases, indicating an improvement in dyes extraction (Fig. 3A). This is attributed to the enhanced diffusion of dyes molecules from the aqueous phase into the TRDES phase due to heating, which reduces DES viscosity and improves mass-transfer kinetics. The value of extraction recovery reached a maximum at 12 min, indicating optimal mass-transfer equilibrium. Beyond this point, extraction recovery remained constant. Thus, 12 min was chosen as the optimal extraction time.

3.2.3. Effect of salting-out agent concentration

The presence of a salting-out agent in the extraction system can reduce the solubility of dyes and TRDES precursors in the aqueous phase, thereby enhancing the efficiency of the HLLME process. Sodium chloride was selected as the salting-out agent due to its low cost and effectiveness. To study its influence, dyes water solutions containing 0, 3, 5, 7, and 9 % NaCl were prepared and used for HLLME (Fig. 3B). At low NaCl concentrations (0–5 %), a gradual increase in the extraction recovery of the dyes in DES phase was observed, suggesting that NaCl promotes dye transfer by reducing the hydration shell of dye molecules and altering aqueous phase polarity. A sharp increase at 7 % NaCl indicates a threshold concentration where enhanced phase separation maximizes extraction efficiency, which is due to the reduction in water-dye interactions, leading to stronger hydrophobic affinity between the dye and DES components. Beyond 7 % NaCl, the extraction efficiency plateaued, likely due to the establishment of mass-transfer equilibrium. Additionally, excessive NaCl may increase the viscosity of the aqueous phase, reducing diffusion, and potentially induce dye aggregation or ion pairing, altering its solubility behavior. For further research, 7 % sodium chloride concentration was used because higher concentrations do not provide a significant increase in extraction efficiency, indicating that the system has reached mass-transfer equilibrium and further adding of salting-out agent is unnecessary.

3.2.4. Effect of pH

The acidity of the aqueous phase can influence the efficiency of mass transfer in liquid–liquid microextraction procedure. The non-alcoholic beverages are predominantly acidic with a few exceptions such as drinking water which may exhibit near-neutral or slightly alkaline pH [27,28]. However, since the present work focuses on the determination of synthetic dyes, the use of pure water as a matrix is not considered relevant. Preliminary studies [11] showed that at strongly acidic pH values (pH = 1–2), the TRDES–water system becomes turbid under ambient conditions due to the protonation of heptanoic acid, a component of the thermos-responsive deep eutectic solvent. This turbidity negatively affects the accuracy and reproducibility of the results. Therefore, the pH range of 3–7 was selected for further investigation. Within this interval, the acidity of the aqueous solution had no significant effect on the extraction efficiency of dyes (Fig. 3C).

3.3. Modeling of the rhodamine extraction into deep eutectic solvent

It should be noted that only Rhodamine 6G was intentionally chosen for MD simulations. This choice was made because the main objective of the work was the development of an automated TRDES-HLLME platform, while MD served only as a supporting tool. Rhodamine, being more polar than Sudan dyes, presented a more challenging extraction case, making it more suitable for modeling key solute–solvent interactions while keeping the primary focus on automation. We

computed the total interaction energy, which encompasses the overall energy of non-bonded contacts, mainly consisting of the sum of van der Waals and electrostatic interaction energies. To comprehend the different pair interactions, specifically rhodamine-lidocaine and rhodamine-heptanoic acid, which are essential for understanding the transfer of rhodamine from the aqueous phase to the organic phase. The van der Waals and electrostatic interaction energies for selected pairs are illustrated in ESM Fig. 3(a) and (b). It is noteworthy that rhodamine-lidocaine is more attractive based on van der Waals and electrostatic interaction energy, as demonstrated in ESM Fig. 3(a) and (b). The average van der Waals interaction energy for rhodamine-lidocaine is -108.94 kCal/mol, while for rhodamine-heptanoic acid, it is -54.42 kCal/mol. This indicates that lower rhodamine-lidocaine energy, i.e., lidocaine plays a vital role in extraction, as evidenced by the π - π interactions with the same pair depicted in ESM Fig. 4. Additionally, we have examined the electrostatic interaction energy between the rhodamine-lidocaine and heptanoic acid pair. The average electrostatic interaction energy for the rhodamine-lidocaine pair is -38.75 kCal/mol, while for rhodamine-heptanoic acid, it is -6.11 kCal/mol.

The trajectory cross-section density is computed by taking layers of a defined thickness perpendicular to the YZ Cartesian coordinate axis. To determine the density profile at a specific point on the axis (referred as the coordinate at the bottom of the layer), the fraction of the van der Waals volume of each atom that overlaps the layer is multiplied by its atomic mass. The results are summed up for all specified atoms and subsequently divided by the volume of the layer. Similarly, for the cross-sectional density, the layer is divided into cubes, and the volume fraction of each atom overlapping each cube is calculated, weighted by the atomic mass, averaged, and divided by the cube volume to yield the density within the cube.

It is evidenced from the trajectory cross-sectional contours that the rhodamine moves from the aqueous phase to the organic phase as shown in ESM Fig. 5. The organic phase region is between 130 and 160 Å in ESM Fig. 5 (a), rhodamine density is maximum within this region, depicting effective separation of 1 wt % of rhodamine from aqueous solution. ESM Fig. 5 (b) shows the cross-sectional density of 5 wt % of rhodamine in aqueous solution-HDES system. The highest density in the contour is evident that rhodamine in organic phase region 100–130 Å shows that higher concentration can be also be effectively separated.

The rhodamine anisotropic diffusion coefficient along the z-direction of aqueous-HDES phase is calculated using the Einstein diffusion Eq.;

$$D = \frac{1}{2} \lim_{t \rightarrow \infty} \frac{d}{dt} \langle |r(t) - r(0)|^2 \rangle$$

Where mean-square displacement is represented by $\langle |r(t) - r(0)|^2 \rangle$, and angled brackets denotes an average value of all the rhodamine molecules. The diffusion coefficients calculated in our investigation are shown in ESM Table 2. There is a clear indication that rhodamine mobility is low along the z-direction in comparison to the other directions, i.e., 1.11×10^{-10} m²/s along the x-direction and 1.11×10^{-10} m²/s along the y-direction. The diffusion coefficient low by three orders of magnitude. This indicate that the rhodamine molecules slowly diffuse along the z-direction from aqueous phase to the organic phase.

To gain insight into the atomistic structure, we computed the radial distribution function (RDF) for rhodamine-lidocaine and rhodamine-heptanoic acid as shown in ESM Fig. 6. The RDF plot was analyzed and indicates that particles are randomly distributed, as demonstrated by g(r) versus radial distance 'r'. g(r) is marginally greater than 1 for rhodamine-heptanoic acid at 6 Å (first neighbor), and g(r) ultimately approaches 1 at longer distances, signifying a lack of correlation beyond 7 Å. Conversely, the rhodamine-lidocaine pair exhibits a broad first neighbor peak at 5 Å, with g(r) thereafter reducing beyond 9 Å, indicating a lack of correlation at longer distances.

3.4. Strategies for online coupling of TRDES-based extraction with HPLC

The integration of automated sample preparation with chromatographic determination represents a key direction in modern analytical chemistry. In the present work, we designed and evaluated three different strategies for coupling the TRDES-based automated microextraction system with HPLC-PDA detection, each providing a different level of automation. These configurations are illustrated in ESM Figs. 7–9 and corresponding demonstration videos (Video 1–3).

The first approach can be described as semi-automated vial filling (ESM Fig. 7, Video 1). In this configuration, following TRDES-based phase separation, the enriched extract is automatically delivered into chromatographic vials positioned in a custom holder compatible with the autosampler. This mode allows online filling of multiple vials, which are subsequently transferred manually as a tray into the HPLC autosampler. From this point onwards, the chromatographic analysis is fully automated. The number of samples prepared in one sequence depends on the number of available valve ports in the multiposition manifold; commercial valves with 12 or more channels make it possible to prepare and analyze more than four samples in parallel. The only manual step in this case is the placement of the vial tray into the autosampler, while all other operations remain automated.

The second approach provides a higher degree of automation by establishing a direct connection between the flow manifold and the injection valve of the HPLC system (ESM Fig. 8, Video 2). Here, the outlet tubing from the extraction chamber is connected via a needle to the dosing valve of the chromatograph. This configuration allows the enriched TRDES phase to be transferred directly into the chromatographic loop without intermediate collection. The current limitation of this setup is that switching of the HPLC injection valve is still performed manually. However, this action can be readily automated by synchronizing valve switching with the extraction sequence. Once implemented, the entire process, from extraction to chromatographic injection, becomes fully automated.

Finally, the third approach represents a fully automated and integrated configuration (ESM Fig. 9, Video 3). In this case, the outlet tubing from the TRDES extraction system is directly inserted through the septum of a vial already positioned in the autosampler tray. The enriched TRDES extract is automatically introduced into the vial, from which it is subsequently aspirated by the autosampler needle for chromatographic injection. This solution enables continuous, unattended operation, as the extract delivery and sampling occur within the same vial and within the same platform. Such an approach provides the highest level of integration, eliminating all manual operations and opening opportunities for long-term, fully automated monitoring.

Taken together, these three coupling strategies demonstrate the feasibility of combining automated TRDES-based sample preparation with chromatographic determination at different levels of technical complexity. While the first two approaches offer straightforward proof-of-concept implementations that can be easily adapted to existing laboratory infrastructure, the third approach represents a path toward fully integrated, online analytical systems.

3.5. Method validation

To evaluate the performance and applicability of the developed TRDES-based microextraction method for the determination of synthetic dyes in food matrices, method validation was carried out according to standard guidelines. The evaluated parameters included linearity, limits of detection (LOD), limits of quantification (LOQ), and intra- and inter-day precision. All experiments were performed for the four target analytes: Rhodamine 6G, Sudan I, Sudan II, and Sudan III. Calibration curves were established using matrix-matched standards prepared by spiking blank food matrices, previously verified to be free of the target dyes, with known analyte concentrations. The validated linear ranges were 0.004–100 mg L⁻¹ for Rhodamine 6G, Sudan I, and Sudan III, and

0.025–100 mg L⁻¹ for Sudan II. All analytes showed excellent linearity, with coefficients of determination (R^2) between 0.9987 and 0.9998. The LOD and LOQ were calculated using signal-to-noise ratios of 3:1 and 10:1, respectively. The LOD values were in the range of 0.001–0.006 mg L⁻¹, while the LOQ values were 0.004–0.025 mg L⁻¹, confirming the method's suitability for trace-level detection of synthetic dyes in food safety applications (Table 2). Precision was assessed at concentration levels (0.1, 5 and 70 mg L⁻¹). Intra-day precision was determined by triplicate analysis within a single day, while inter-day precision was evaluated over three consecutive days (Table 3). The relative standard deviations (RSDs) ranged from 3.0 % to 4.0 % for intra-day measurements and from 5.0 % to 7.0 % for inter-day measurements, depending on the analyte and concentration. These results demonstrate good repeatability and reproducibility of the developed procedure. The recoveries of the analytes ranged from 89 % to 96 %, corresponding to enrichment factors between 21 and 23. Specifically, the enrichment factor was 21 for Rhodamine 6G, 22 for Sudan I, 22 for Sudan II, and 23 for Sudan III, reflecting the higher affinity of the Sudan dyes for the nonpolar TRDES phase compared to the more polar Rhodamine 6G. The trueness of the method was evaluated by recovery studies in real beverage matrices and comparison with a DLLME-HPLC method [22]. As both approaches rely on similar extraction and chromatographic principles, this assessment should be regarded as preliminary. Certified reference materials for synthetic dyes in beverages are not commercially available; therefore, future work will focus on validating trueness against CRMs or independent methods based on different analytical principles, in accordance with the Eurachem Guide (3rd ed., 2025).

3.6. Analysis of real sample

To demonstrate the practical applicability of the developed method, it was applied to the analysis of three commercially available beverages (cherry juice, lemonade, and tonic water). All samples were processed directly using the automated TRDES-based microextraction system according to the optimized procedure. None of the dyes were detected above the method's LOD in the original samples; therefore, only the results obtained for spiked samples at two concentration levels (0.10 and 5.00 mg L⁻¹) are reported (Table 4). The spiked samples were independently analyzed by a validated reference DLLME-HPLC method in order to assess the accuracy of the TRDES-based procedure. The results obtained with the two methods showed excellent agreement. Statistical evaluation using the Student's t-test and F-test at the 95 % confidence level confirmed the absence of significant differences between the methods. The relative bias for spiked samples remained within 1–5 %, demonstrating that the developed approach provides accurate and reliable quantification across both low and medium concentration ranges. These findings confirm that the automated TRDES-HLLME method is suitable for routine screening and quantification of banned dyes in beverage matrices, offering analytical reliability together with automation and reduced solvent consumption.

3.7. Assessment of greenness

The environmental friendliness of the developed procedure for the dyes determination in food samples was assessed using the AGREEprep

Table 2
Validated features of the developed procedure.

Analyte	Linear range (mg L ⁻¹)	R ²	LOD (mg L ⁻¹)	LOQ (mg L ⁻¹)	Recovery (%)	EF
Rhodamine 6G	0.004–100	0.9998	0.001	0.004	92	21
Sudan I	0.025–100	0.9998	0.006	0.025	94	22
Sudan II	0.004–100	0.9998	0.001	0.004	96	22
Sudan III	0.004–100	0.9987	0.001	0.004	89	23

Table 3

Intra- and inter-day precision (RSD, %, n = 3) and accuracy (%) for QC samples at three levels.

Analyte	QC level (mg L ⁻¹)	Intra-day RSD (%)	Inter-day RSD (%)	Accuracy (%)
Rhodamine 6G	0.10	4.20	6.30	92.50
	5.00	3.00	6.00	94.00
	70.00	2.30	4.00	96.00
Sudan I	0.10	4.80	7.20	91.00
	5.00	4.00	7.00	93.50
	70.00	3.00	5.00	95.00
Sudan II	0.10	5.00	7.50	90.00
	5.00	4.10	7.00	93.00
	70.00	3.20	5.00	95.50
Sudan III	0.10	4.90	7.30	91.50
	5.00	4.00	7.00	94.00
	70.00	3.10	5.00	96.50

and ComplexGAPI metrics [29]. The AGREEprep metric evaluates ten criteria, including reagent sustainability, waste generation, sample mass/volume, and automation use [30]. The overall eco-friendliness of the sample preparation process was assessed using AGREEprep and visualized as a colorful round pictogram with a numeric value in the center. The method achieved an overall score of 0.73, confirming its good green profile (ESM Fig. 10). Scores range from 0 to 1, with 1 representing full compliance with green chemistry principles.

The Complex Green Analytical Procedure Index (ComplexGAPI) is a comprehensive metric for evaluating the environmental sustainability of analytical methodologies. This metric accounts not only for the analytical procedure itself but also for pre-analytical processes used in the method. The metric is visualized as a pictogram with color-coded fields reflecting various parameters (ESM Fig. 11). The main factors reducing the eco-friendliness of the procedure are the use of the HPLC-PDA system which has disadvantages such as high-energy consumption and use of toxic solvents as a mobile phase, and off-line sample preparation. Despite these disadvantages, the overall environmental friendliness of the developed procedure is much higher than that of traditional procedures due to small amounts, no preservation of samples and their simple storage. In addition to its eco-friendliness, an important aspect of

this methodology is its practicality. This approach is automated, which significantly increases throughput, reducing energy consumption and minimizing human errors.

3.8. Comparison with existing methods

Compared to existing analytical approaches for the determination of synthetic dyes in food products, the proposed method offers several significant advantages in terms of green chemistry, operational simplicity, and analytical performance. Most conventional methods rely on organic solvent-based liquid-liquid extraction (LLE) [21,31], solid-phase extraction (SPE) [21], or dispersive solid-phase extraction (d-SPE) followed by chromatographic determination. While effective, these techniques typically involve multiple manual steps, require large volumes of organic solvents [32,33], and are often matrix-dependent, requiring separate optimization for different types of food products. Furthermore, they are not easily adaptable to automation and may exhibit limited reproducibility when scaled up for high-throughput screening [34,35].

In contrast, the developed method utilizes a homogeneous aqueous solution of a temperature-responsive deep eutectic solvent as a universal extraction medium. This system eliminates the need for conventional organic solvents and offers selective, thermally driven phase separation upon heating (ESM Table 3). Another major strength of the method is its compatibility with complex liquid matrices without requiring significant modification of the procedure. The same TRDES composition and volume were successfully used for the extraction of dyes from various beverages, demonstrating the method's versatility and consistent performance across different matrices. Additionally, the entire procedure was integrated into an automated, flow-based platform capable of performing all steps, including TRDES delivery, extraction, phase separation, and sample collection, without manual intervention. This complete automation improves method accuracy, reduces operator workload, and enables high-throughput analysis suitable for routine food control laboratories.

Finally, the method is characterized by low consumption of TRDES (only 250 µL per analysis), minimizing chemical waste and aligning with

Table 4

Determination of dyes in real samples (n = 3, P = 0.95, t = 2.78, F = 19.00).

Sample	Dye	Added (mg L ⁻¹)	Found Proposed method (mg L ⁻¹ , mean ± SD, n = 3)	Found Reference method (mg L ⁻¹ , mean ± SD, n = 3)	t-test	F-test	Relative bias (%)
Cherry juice	Sudan I	0.1	0.093 ± 0.006	0.090 ± 0.005	0.92	1.44	7
		5	4.84 ± 0.15	4.65 ± 0.18	1.4	1.49	3.2
	Sudan II	0.1	0.098 ± 0.007	0.095 ± 0.006	0.87	1.36	2
		5	4.91 ± 0.17	4.72 ± 0.12	1.58	2.01	1.8
	Sudan III	0.1	0.101 ± 0.006	0.097 ± 0.007	1.12	1.27	1
		5	4.92 ± 0.16	4.76 ± 0.14	1.3	1.31	1.6
Lemonade	Rhodamine 6G	0.1	0.094 ± 0.005	0.096 ± 0.006	0.73	1.2	6
		5	4.69 ± 0.14	4.77 ± 0.20	0.53	1.38	6.2
	Sudan I	0.1	0.102 ± 0.008	0.099 ± 0.007	0.81	1.31	2
		5	5.05 ± 0.16	4.83 ± 0.15	1.74	1.14	1
	Sudan II	0.1	0.095 ± 0.006	0.097 ± 0.005	0.67	1.25	5
		5	4.69 ± 0.14	4.74 ± 0.17	0.39	1.47	6.2
Sudan III	0.1	0.098 ± 0.007	0.096 ± 0.006	0.88	1.33	2	
	5	4.72 ± 0.14	4.92 ± 0.15	1.69	1.15	5.6	
Tonic water	Rhodamine 6G	0.1	0.099 ± 0.006	0.097 ± 0.007	0.92	1.29	1
		5	5.10 ± 0.13	5.25 ± 0.15	1.31	1.33	2
	Sudan I	0.1	0.096 ± 0.007	0.093 ± 0.006	0.89	1.36	4
		5	4.82 ± 0.14	4.94 ± 0.17	0.94	1.47	3.6
	Sudan II	0.1	0.097 ± 0.005	0.095 ± 0.006	0.69	1.21	3
		5	4.87 ± 0.13	5.02 ± 0.14	1.36	1.16	2.6
Sudan III	0.1	0.101 ± 0.006	0.098 ± 0.007	0.95	1.35	-1	
	5	5.25 ± 0.15	5.00 ± 0.22	1.63	2.15	-5	
Rhodamine 6G	0.1	0.094 ± 0.007	0.096 ± 0.006	0.71	1.17	6	
	5	4.77 ± 0.16	4.96 ± 0.14	1.55	1.31	4.6	

the principles of green analytical chemistry. The extractant can be prepared in advance, is stable under storage, and does not require regeneration or complex cleanup procedures. Taken together, these features distinguish the proposed method as a novel, efficient, and environmentally friendly alternative to traditional dye extraction protocols, particularly well-suited for modern, automated laboratories focused on the screening of banned substances in complex liquid food matrices.

4. Conclusions

In this study, a automated microextraction method was developed for the determination of synthetic food dyes using temperature-responsive deep eutectic solvents. The key innovation lies in the use of a homogeneous aqueous TRDES solution, which acts as both extraction medium and thermally induced phase-separating agent. This dual function significantly simplifies sample handling and eliminates the need for organic solvents or centrifugation, a common limitation in existing TRDES protocols. The method was thoroughly optimized for liquid samples. Critical parameters such as extraction time, temperature, sample amount, and extraction mode were systematically optimized to maximize recovery and phase stability. Validation of the method demonstrated its suitability for quantitative analysis of four structurally diverse banned dyes. The procedure exhibited excellent linearity, low detection limits, and high accuracy in both intra-day and inter-day analyses. Application to real food samples confirmed the method's reliability: none of the dyes were detected in beverage samples, and the results of spiked recovery tests showed high agreement with those obtained using a validated reference method. Statistical evaluation using t- and F-tests further confirmed the comparability of the proposed and standard techniques. Beyond its analytical performance, the method's most impactful advantage is its automation. All critical steps from solvent delivery to extractant recovery were integrated into a programmable flow-based platform. The system uses only 250 μL of TRDES per run, aligning with green chemistry principles by reducing solvent waste and operator exposure. The interaction energy calculations suggest that the rhodamine-lidocaine are strongly attractive in comparison to the rhodamine-heptanoic acid. The π - π interactions between the rhodamine-lidocaine dominate and responsible for the extraction of the rhodamine from water phase to organic phase. The diffusion coefficient along the z-direction is low by the three orders of magnitude indicate the resistance at the interface.

Overall, the proposed method provides a robust, selective, and sustainable solution for the determination of synthetic dyes in complex food matrices. It represents a substantial step forward in the field of automated green sample preparation and holds strong potential for routine application in food quality and safety control laboratories.

The present work thus constitutes the first demonstration of an automated TRDES-HLLME platform. By combining thermally induced phase separation with flow-based automation, the method not only improves analytical performance but also advances the field of green sample preparation, providing a foundation for future high-throughput applications in food safety monitoring. The real-world relevance of the developed method lies in its potential use for routine monitoring of banned synthetic dyes in food and beverages by food control laboratories, regulatory agencies, and quality assurance units. The integration of TRDES-based extraction with automated flow handling significantly reduces operator involvement, increases reproducibility, and minimizes the use of hazardous solvents. These features make the approach particularly suitable for high-throughput screening in compliance testing and routine quality control, thereby supporting regulatory frameworks for food safety.

CRedit authorship contribution statement

Alesia Gerasimova: Investigation. **Anoop Kishore Vatti:** Writing – original draft, Investigation. **Tamal Banerjee:** Writing – original draft,

Investigation. **Andrey Shishov:** Writing – original draft, Investigation, Conceptualization.

Declaration of competing interest

The authors declare that they have no known competing financial interests or personal relationships that could have appeared to influence the work reported in this paper.

Acknowledgements

Andrey Shishov gratefully acknowledges financial support of Russian Science Foundation (research projects No. 24-43-02023). Scientific research was performed using the equipment of the Research Parks of St. Petersburg State University (Chemical Analysis and Materials Research Centre, Centre of Thermal Analysis and Calorimetry and cryogenic department of the Scientific Park of St. Petersburg State University). Tamal Banerjee acknowledges the approval of funding vide DST/IC/RSF/2024/333 under International Cooperation Division under India-Russia Joint Research Call Scheme. We would also like to thank the PARAM KAMRUPA supercomputer for its computational time and Schrödinger Centre for Molecular Simulations, Manipal Academy of Higher Education (MAHE), Manipal for their support.

Appendix A. Supplementary data

Supplementary data to this article can be found online at <https://doi.org/10.1016/j.talanta.2025.129029>.

Data availability

Data will be made available on request.

References

- [1] A.V. Kozhevnikova, E.S. Uvarova, V.E. Maltseva, I.V. Ananyev, N.A. Milevskii, I. S. Fedulov, Y.A. Zakhodyaeva, A.A. Voshkin, Design of eutectic solvents with specified extraction properties based on intermolecular interaction energy, *Molecules* 29 (2024) 5022, <https://doi.org/10.3390/molecules29215022>.
- [2] B. Hosseinezhad, M. Nemati, M.A. Farajzadeh, E. Marzi Khosrowshahi, M. R. Afshar Mogaddam, Deep eutectic solvent applications in sample preparation of different analytes before gas and liquid chromatography instruments coupled with mass spectrometry and tandem mass spectrometry, *TrAC, Trends Anal. Chem.* 169 (2023) 117346, <https://doi.org/10.1016/j.trac.2023.117346>.
- [3] N. Tsvetov, O. Paukshta, N. Fokina, N. Volodina, A. Samarov, Application of natural deep eutectic solvents for extraction of bioactive components from *Rhodiola rosea* (L.), *Molecules* 28 (2023) 912, <https://doi.org/10.3390/molecules28020912>.
- [4] V. Andrich, V. Vojteková, A. Kalyniukova, G. Zengin, I. Hagarová, T. Yordanova, Application of deep eutectic solvents for the determination of inorganic analytes, *Adv. Sample Prep.* 13 (2025) 100158, <https://doi.org/10.1016/j.sampre.2025.100158>.
- [5] M. Nemati, M. Tuzen, N. Altunay, M.A. Farajzadeh, F. Abdi, M.R. Afshar Mogaddam, Development of sodium hydroxide-induced homogenous liquid-liquid extraction–effervescent assisted dispersive liquid-liquid microextraction based on deep eutectic solvents; application in the extraction of phytosterols from cow cream samples, *J. Food Compos. Anal.* 106 (2022) 104291, <https://doi.org/10.1016/j.jfca.2021.104291>.
- [6] F.C. Pouget, J.-M. Andanson, A. Gautier, Thermo-switchable hydrophobic deep eutectic solvent for CuAAC, *RSC Sustain.* 1 (2023) 1826–1832, <https://doi.org/10.1039/D3SU00249G>.
- [7] D. Xiong, Q. Zhang, W. Ma, Y. Wang, W. Wan, Y. Shi, J. Wang, Temperature-switchable deep eutectic solvents for selective separation of aromatic amino acids in water, *Sep. Purif. Technol.* 265 (2021) 118479, <https://doi.org/10.1016/j.seppur.2021.118479>.
- [8] O. Longeras, A. Gautier, K. Ballerat-Busserolles, J.-M. Andanson, Deep eutectic solvent with thermo-switchable hydrophobicity, *ACS Sustain. Chem. Eng.* 8 (2020) 12516–12520, <https://doi.org/10.1021/acsschemeng.0c03478>.
- [9] B. Shiquan, R. Sun, P. Zhou, Y. Li, X. Shang, Temperature-responsive deep eutectic solvent as eco-friendly and recyclable media for the rapid assessment of pyrethroid pesticide residues in surface soil sample, *Microchem. J.* 181 (2022) 107733, <https://doi.org/10.1016/j.microc.2022.107733>.
- [10] L. Shen, Y. Yan, X. Jiang, X. Yang, Z. Zhang, Z. Li, Ultrasound-assisted ternary temperature-responsive deep eutectic solvents for extraction of carotenoids from tomato samples, *Food Chem.* 473 (2025) 143065, <https://doi.org/10.1016/j.foodchem.2025.143065>.

- [11] P. Godunov, A. Gerasimova, A. Shishov, A. Bulatov, Temperature-responsive deep eutectic solvent-based microextraction for the determination of bisphenols in beverages by HPLC-FLD, *J. Food Compos. Anal.* 135 (2024) 106569, <https://doi.org/10.1016/j.jfca.2024.106569>.
- [12] J. Castaneda Corzo, K. Ballerat-Busserolles, J.-Y. Coxam, A. Gautier, J.-M. Andanson, Thermo-switchable hydrophobic solvents formulated with weak acid and base for greener separation processes, *J. Mol. Liq.* 377 (2023) 121468, <https://doi.org/10.1016/j.molliq.2023.121468>.
- [13] F. Tissot, J.C. Rodríguez, L. Gutiérrez, Online flow-batch dispersive liquid-liquid microextraction system for ET AAS determination of molybdenum in water and complex matrices, *J. Anal. Chem.* 79 (2024) 1450–1458, <https://doi.org/10.1134/S1061934824700837>.
- [14] I.I. Timofeeva, K.A. Barbayanov, A.V. Bulatov, Automated liquid-liquid microextraction of fluoroquinolones for their subsequent chromatographic determination, *J. Anal. Chem.* 78 (2023) 207–212, <https://doi.org/10.1134/S1061934823020132>.
- [15] H. Sulistyarti, L.A. Putri, V. Suryani, R. Retnowati, U. Andayani, A. Mulyasuryani, E. Sulisty, M.M. Utama, A green approach to ammonia determination in human saliva using natural reagent via gas-diffusion flow-injection spectrophotometry, *J. Anal. Chem.* 79 (2024) 1747–1756, <https://doi.org/10.1134/S1061934824701314>.
- [16] S. Yildirim, D.J. Cocovi-Solberg, B. Uslu, P. Solich, B. Horstkotte, Lab-in-syringe automation of deep eutectic solvent-based direct immersion single drop microextraction coupled online to high-performance liquid chromatography for the determination of fluoroquinolones, *Talanta* 246 (2022) 123476, <https://doi.org/10.1016/j.talanta.2022.123476>.
- [17] R. Muradymov, N. Paul, N. Kumar Das, T. Banerjee, A. Shishov, Quasi-hydrophobic deep eutectic solvents for simultaneous automated determination of polar and non-polar dyes in food products, *Microchem. J.* 206 (2024) 111510, <https://doi.org/10.1016/j.microc.2024.111510>.
- [18] P. Upadhyay, P. Bhaskar, R. Datla, Detection of carcinogenic dye Sudan I and Rhodamine B using indigenous Raman spectrometer, *Asian Pac. J. Health Sci.* 9 (2022) 280–283, <https://doi.org/10.21276/apjhs.2022.9.4S.53>.
- [19] I. Kruglenko, J. Burlachenko, B. Snopok, Interaction of the fluorescent cell-labeling dye Rhodamine 6G with low-molecular-weight compounds: a comparative QCM study of adsorption capacity of Rh6G for gaseous analytes, in: *Proc. 10th Int. Electron. Conf. Sensors Appl.*, 2023, p. 115, <https://doi.org/10.3390/ecsa-10-16200>.
- [20] D. Zhang, H. Pu, L. Huang, D.-W. Sun, Advances in flexible surface-enhanced Raman scattering (SERS) substrates for nondestructive food detection: fundamentals and recent applications, *Trends Food Sci. Technol.* 109 (2021) 690–701, <https://doi.org/10.1016/j.tifs.2021.01.058>.
- [21] R. Rebane, I. Leito, S. Yurchenko, K. Herodes, A review of analytical techniques for determination of Sudan I–IV dyes in food matrices, *J. Chromatogr. A* 1217 (2010) 2747–2757, <https://doi.org/10.1016/j.chroma.2010.02.038>.
- [22] P. Biparva, E. Ranjbari, M.R. Hadjmohammadi, Application of dispersive liquid-liquid microextraction and spectrophotometric detection to the rapid determination of rhodamine 6G in industrial effluents, *Anal. Chim. Acta* 674 (2010) 206–210, <https://doi.org/10.1016/j.aca.2010.06.024>.
- [23] K.J. Bowers, D.E. Chow, H. Xu, R.O. Dror, M.P. Eastwood, B.A. Gregersen, J. Klepeis, I. Kolossvary, M.A. Moraes, F.D. Sacerdoti, J.K. Salmon, Y. Shan, D. E. Shaw, Scalable algorithms for molecular dynamics simulations on commodity clusters, *Proc. ACM/IEEE SC Conf.* (2006), <https://doi.org/10.1109/SC.2006.54>.
- [24] C. Lu, C. Wu, D. Ghoreishi, W. Chen, L. Wang, W. Damm, G.A. Ross, M.K. Dahlgren, E. Russell, C.D. Von Bargen, R. Abel, R.A. Friesner, E.D. Harder, OPLS4: improving force field accuracy on challenging regimes of chemical space, *J. Chem. Theor. Comput.* 17 (2021) 4291–4300, <https://doi.org/10.1021/acs.jctc.1c00302>.
- [25] U. Essmann, L. Perera, M.L. Berkowitz, T. Darden, H. Lee, L.G. Pedersen, A smooth particle mesh Ewald method, *J. Chem. Phys.* 103 (1995) 8577–8593, <https://doi.org/10.1063/1.470117>.
- [26] T. Darden, D. York, L. Pedersen, Particle mesh Ewald: an N-log(N) method for Ewald sums in large systems, *J. Chem. Phys.* 98 (1993) 10089–10092, <https://doi.org/10.1063/1.464397>.
- [27] A. Reddy, D.F. Norris, S.S. Momeni, B. Waldo, J.D. Ruby, The pH of beverages in the United States, *J. Am. Dent. Assoc.* 147 (2016) 255–263, <https://doi.org/10.1016/j.adaj.2015.10.019>.
- [28] D. Birkhed, Sugar content, acidity and effect on plaque pH of fruit juices, fruit drinks, carbonated beverages and sport drinks, *Caries Res.* 18 (1984) 120–127, <https://doi.org/10.1159/000260759>.
- [29] A.Y. Shishov, O.B. Mokhodoeva, Green chemistry metrics in analytical chemistry, *J. Anal. Chem.* 79 (2024) 487–499, <https://doi.org/10.1134/S1061934824050125>.
- [30] L.A. Yahya, C. Vakh, O. Dushna, O. Kalisz, S. Bocian, M. Tobiszewski, Guidelines on the proper selection of greenness and related metric tools in analytical chemistry – a tutorial, *Anal. Chim. Acta* 1357 (2025) 344052, <https://doi.org/10.1016/j.aca.2025.344052>.
- [31] R. Du, Y. Zhang, Y. Bian, C. Yang, X. Feng, Z. He, Rhodamine and related substances in food: recent updates on pretreatment and analysis methods, *Food Chem.* 459 (2024) 140384, <https://doi.org/10.1016/j.foodchem.2024.140384>.
- [32] M.E. Machado, M.M. Nascimento, P.V. Bomfim Bahia, S.T. Martinez, J. Bittencourt De Andrade, Analytical advances and challenges for the determination of heterocyclic aromatic compounds (NSO-HET) in sediment: a review, *TrAC, Trends Anal. Chem.* 150 (2022) 116586, <https://doi.org/10.1016/j.trac.2022.116586>.
- [33] W. Zhou, M.N. Wiecezorek, H. Javanmardi, J. Pawliszyn, Direct solid-phase microextraction–mass spectrometry facilitates rapid analysis and green analytical chemistry, *TrAC, Trends Anal. Chem.* 166 (2023) 117167, <https://doi.org/10.1016/j.trac.2023.117167>.
- [34] A. Shishov, U. Markova, V. Mulloyarova, P. Tolstoy, N. Shkaeva, D. Kosyakov, N. K. Das, T. Banerjee, Deep eutectic solvent as stationary phase for flow analysis: automated trace metal determination in food products, *Anal. Chim. Acta* 1332 (2024) 343356, <https://doi.org/10.1016/j.aca.2024.343356>.
- [35] D.A. Vargas Medina, E.V.S. Maciel, F.M. Lanças, Modern automated sample preparation for the determination of organic compounds: a review on robotic and on-flow systems, *TrAC, Trends Anal. Chem.* 166 (2023) 117171, <https://doi.org/10.1016/j.trac.2023.117171>.